

Cite this article as: Hou Jijun, Dong Junhui, Xu Aiping. Weld Formation, Microstructure and Mechanical Properties of Laser Welded TC4 Titanium Alloy with Activating Fluxes[J]. Rare Metal Materials and Engineering, 2021, 50(12): 4236-4244.

ARTICLE

# Weld Formation, Microstructure and Mechanical Properties of Laser Welded TC4 Titanium Alloy with Activating Fluxes

Hou Jijun, Dong Junhui, Xu Aiping

School of Materials Science and Engineering, Inner Mongolia University of Technology, Hohhot 010051, China

**Abstract:**  $\text{CaF}_2$ ,  $\text{NaF}$  and  $\text{Na}_2\text{SiF}_6$  were chosen as activating fluxes for laser welding of Ti6Al4V (TC4) alloy. During the welding process, the laser-induced plasma images above the weldment were captured with a high-speed camera. After welding, the weld penetration and the width of the weld were measured and the microstructure was observed by an optical microscope. Then, the morphology of acicular martensite in the weld was studied by EBSD, and the element composition of the weld was determined by energy spectrometer. The hardness and tensile strength of the joints were tested. The results show that the activating fluxes change the surface state of the weldment and compress the laser-induced plasma area, thereby increasing the laser absorptivity and the area of the weld melting zone. Besides, all the activating fluxes can increase the penetration depth and reduce the top weld width of the partial penetration weld, and reduce the top weld width while increase the middle and bottom weld widths of the penetration weld. It is also found that for the welds coated with  $\text{CaF}_2$ ,  $\text{NaF}$  and without activating fluxes, the  $\beta$  columnar crystals on the upper part of the welds all grow towards the weld surface, while for the welds coated with  $\text{Na}_2\text{SiF}_6$ , the  $\beta$  columnar crystals on the upper part of the welds grow towards the weld center. The activating fluxes have no obvious effect on the growing direction of the  $\beta$  columnar crystals of the lower part of the weld.  $\text{Na}_2\text{SiF}_6$  can significantly refine the acicular  $\alpha'$  in the  $\beta$  columnar crystals of the upper part of the welds in the laser welding of TC4 alloy. The tensile strength of the welded joint coated with  $\text{Na}_2\text{SiF}_6$  is increased by 12.5%. Compared with other activating fluxes,  $\text{Na}_2\text{SiF}_6$  has the most prominent effect on the weld formation and mechanical property of the laser welded TC4 titanium alloy, and thus it can be used as the most preferred activating flux.

**Key words:** activating flux; TC4; weld formation; microstructure; mechanical property

Titanium alloy is widely used in the aerospace, medical fields<sup>[1,2]</sup> as well as shipbuilding industry<sup>[3]</sup> due to its high specific strength, excellent biocompatibility and strong corrosion resistance, respectively. However, the welded joint of titanium alloy is easily overheated, thus resulting in coarse microstructure and wide heat affected zone, because of its high melting point and low thermal conductivity. It is difficult to solve these problems effectively by traditional arc welding with low energy density. Comparatively, laser welding with high energy density may be able to do. It is shown that the laser welded joints of TC4 titanium alloy welded by LBW (laser beam welding), EBW (electron beam welding) and TIG (tungsten insert gas welding) have the narrowest weld bead, the least deformation and the finest grain<sup>[4,5]</sup>.

However, laser welding has its own defect, i. e., the laser energy loss caused by reflection. In order to save the energy,

some scholars inspired by A-TIG coated the workpiece with activating fluxes before welding. Among them, Kaul<sup>[6]</sup> selected  $\text{SiO}_2$  as the activating flux for the laser welding of 304 stainless, which was proven to significantly change the shape of the fusion zone so that more energy was saved, and narrower and deeper welds were produced. Besides, it is found that other activating fluxes have the similar effect on weld formation<sup>[7-9]</sup>. Activating fluxes have also been successfully applied in laser welding of alloys such as aluminum alloy and magnesium alloy<sup>[10-14]</sup>, but research on their application to titanium alloy is rarely involved. Plus, former studies on laser welding with activating flux mainly focused on the effect of flux on weld formation, and there is little research on its microstructure. Therefore, to fill the gaps in previous studies, this research selected  $\text{CaF}_2$ ,  $\text{NaF}$  and  $\text{Na}_2\text{SiF}_6$  which were once applied in A-TIG or other welding

Received date: December 13, 2020

Foundation item: National Natural Science Foundation of China (51165027)

Corresponding author: Dong Junhui, Ph. D., Professor, School of Materials Science and Engineering, Inner Mongolia University of Technology, Hohhot 010051, P. R. China, Tel: 0086-471-6575752, E-mail: jhdong@imut.edu.cn

Copyright © 2021, Northwest Institute for Nonferrous Metal Research. Published by Science Press. All rights reserved.

techniques<sup>[15-17]</sup> as activating fluxes for the laser welding of TC4 titanium alloy, and explored the effect of the activating fluxes on the weld formation and microstructure of the weld. The mechanism of the activating fluxes in the welding process of TC4 titanium alloy was also explored.

### 1 Experiment

TC4 titanium alloy plates were extracted from a hot-rolled structural plate. The size of self-fusion welding plates was 140 mm×45 mm×5 mm, and that of butt welding plates was 120 mm×90 mm×5 mm. Fig. 1 shows the room-temperature microstructure of TC4 titanium alloy, which consists of  $\alpha$  and  $\beta$  phases, and the white area represents the  $\alpha$  phase and the black is the  $\beta$  phase. Some  $\alpha$  phases are equiaxed while others are in irregular block shape.  $\beta$  phases are distributed at the grain boundary of  $\alpha$  phase.

Before welding, mechanical and chemical cleanings were conducted to remove impurities and oxide films on the surface. Then, each activating flux, including  $\text{CaF}_2$ ,  $\text{NaF}$  and  $\text{Na}_2\text{SiF}_6$ , was uniformly sprinkled on the plate by a self-made funnel screen with a nickel foam bottom, as shown in Fig. 2. They all covered half of the plate, and the thickness of the flux was ensured to completely cover the surface of the plate. The width of coating on both sides of butt plate was about 15 mm. After that, acetone was dropped slowly on the side of the plate covered with the flux until the flux was completely soaked by it. Plates coated with fluxes are shown in Fig. 3.

Workpieces shown in Fig. 3 were then welded by YLS-10000 fiber laser produced by IPG Company with the laser power of 3000 and 3500 W. The welding direction is presented by the arrows in Fig. 3. The workpieces were welded

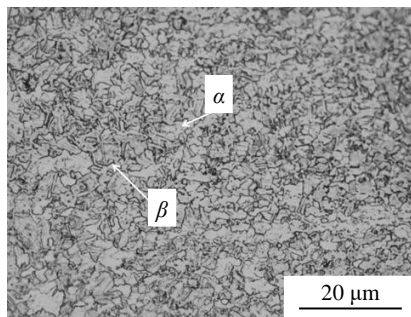


Fig.1 Microstructure of TC4 titanium alloy

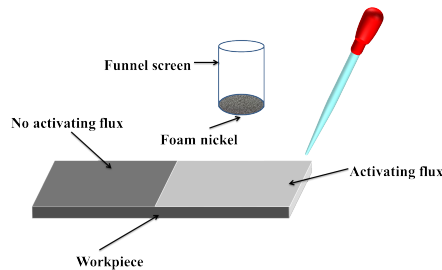


Fig.2 Schematic diagram of coating with activating flux

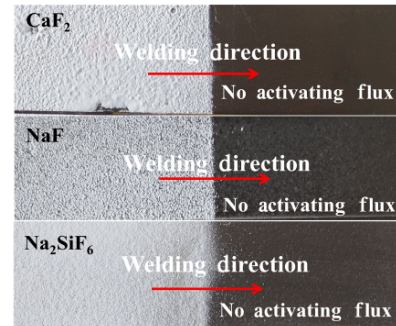


Fig.3 Plates coated with activating fluxes

with the same welding speed, defocusing quantity and argon flow rate, which were 0.03 mm/s, 0 mm and 15 L/min, respectively.

The 5 mm thick uncoated butt plate was welded at laser power of 3300 W; after that the activating fluxes were applied at laser power of 3200 W. The welding speed and defocusing quantity were 0.035 mm/s, and 0 mm, respectively, and the argon flow rates of front shielding gas and back shielding were 15 and 10 L/min, respectively.

During the welding process, the laser-induced plasma images above the weldment were captured with a high-speed camera (BaumerHXC13). After polishing and etching the welds, the size of them, including the weld penetration ( $H$ ), the top weld width ( $W_T$ ), the middle weld width ( $W_M$ ), and the bottom weld width ( $W_B$ ), and the fusion area ( $S$ ), was measured by an optical microscope (ZEISS Stemi 2000-C) using the method shown in Fig.4. Then, the microstructure of the welds was observed with ZEISS Axio Imager optical microscope. The tensile properties of the joint were tested by the universal testing machine 5HT4605, and the hardness of the joint was tested with the digital Vickers hardness tester HXD-1000TM.

### 2 Results and Discussion

#### 2.1 Weld formation

Fig. 5 demonstrates the macro morphologies of each weld when the laser power is 3000 W. It can be observed that the continuity and uniformity of the top welds are not significantly deteriorated due to the activating fluxes. Moreover, compared with the welds without activating fluxes, judging from the color of the weld surface, the welds coated

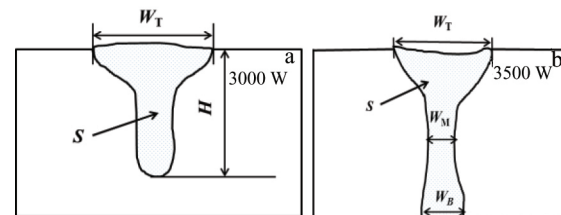


Fig.4 Schematic diagrams of weld size measurement at 3000 W (a) and 3500 W (b)

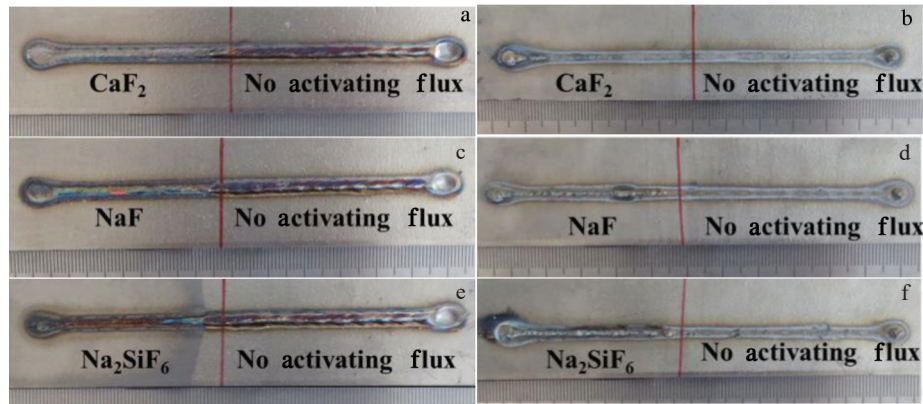


Fig.5 Macro morphologies of welds: (a, c, e) front weld and (b, d, f) back weld

with fluxes do not undergo obvious oxidation. Besides, it can be found from the back of the workpieces that the welds coated with NaF and  $\text{Na}_2\text{SiF}_6$  are almost completely penetrated, and the weld coated with  $\text{CaF}_2$  is penetrated in some areas, but the welds without activating fluxes do not undergo any penetration. However, when the laser power is increased to 3500 W, the welds on both sides coated with or without activating fluxes are completely penetrated. Since no obvious difference in the morphology of these welds is visually observed, the weld images are not shown in this paper.

Fig. 6 presents the size of each weld when welded at the laser power of 3000 and 3500 W. It can be seen that the welds with activating fluxes have a deeper penetration than the welds without fluxes. What's more, the width of the top welds with activating fluxes is smaller than that of the welds without fluxes. According to Fig. 6a, the minimum top weld width of 2.557 mm appears on the welds coated with  $\text{Na}_2\text{SiF}_6$ . As mentioned above, when the laser power is increased to 3500 W, the welds are fully penetrated whether the activating fluxes are applied or not. According to Fig. 6b, the top width of the welds with activating fluxes is also smaller than that of the welds without fluxes, but the middle and the bottom widths of them are larger than those of the welds without fluxes. For the weld coated with  $\text{Na}_2\text{SiF}_6$ , its top width is the smallest, 2.784 mm, while its middle and bottom width are the largest, 1.538

and 1.869 mm, respectively. Obviously, the depth-to-width ratio ( $R=H/W_T$ ) of the welds is increased. The physical quantity of the ratio of the bottom width to the top width is defined as  $R_w=W_B/W_T$  to quantitatively characterize the weld shape.

Fig. 7 shows the effect of activating fluxes on  $R$  and  $R_w$ . It is clear that the depth-to-width ratio ( $R=H/W_T$ ) of the welds is increased, and the  $R_w$  of the welds with activating fluxes is higher than that of the welds without fluxes. These results indicate that it is easier to obtain a weld with a deeper, narrower and more symmetrical shape after being coated with three activating fluxes and  $\text{Na}_2\text{SiF}_6$  has the most obvious effect on weld formation among them.

Fig. 8 shows that the melting area of the welds coated with activating fluxes is larger than that of the welds without fluxes, suggesting that the activating fluxes can increase the laser absorptivity.

## 2.2 Mechanism of activating laser welding

The laser absorptivity is related to the surface condition of the workpiece, such as roughness and coating. The coating of the workpiece directly affects the reflection of the laser. The smoother the surface, the higher the reflectivity. Besides, activating fluxes coated on the surface of the workpiece will increase the surface roughness. Zhang's research<sup>[18]</sup> indicates that because the increase in the number of rays is related to the enhancement of multiple reflections between powders, the

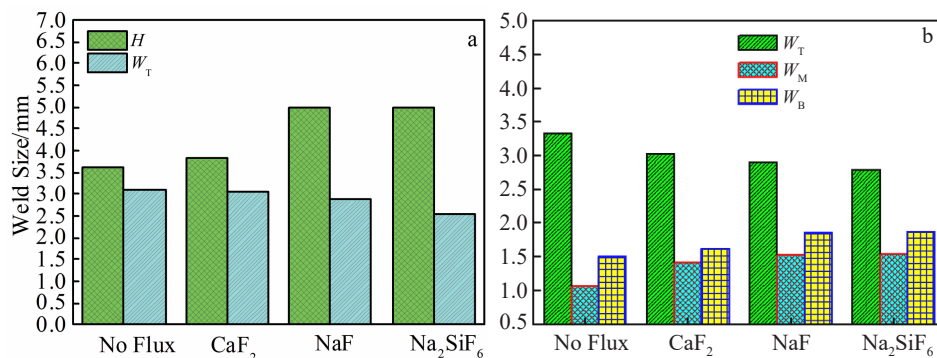


Fig.6 Penetration and width of the welds at the power of 3000 W (a) and 3500 W (b)

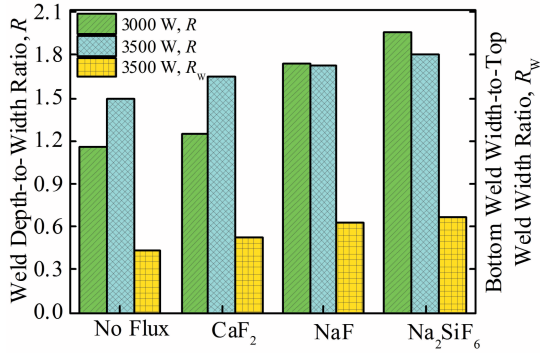


Fig.7 R and  $R_w$  of welds with and without activating fluxes

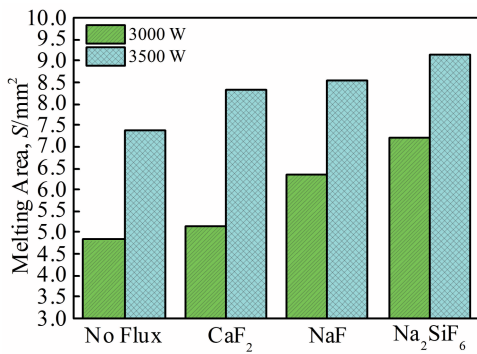


Fig.8 Melting area of welds with and without activating fluxes

absorptivity of the powder layers considerably exceeds the value of a single powder particle or a dense solid material. Fig.9<sup>[19]</sup> shows that the laser beam can be reflected multiple times in powder particles, which means that the laser beam reflected into the air is reduced. What's more, laser absorptivity is also related to the laser-induced plasma which can block the incoming laser beam, thereby reducing the penetration. This phenomenon is usually referred to as the shielding effect of the plasma<sup>[7]</sup>.

Fig.10 shows that the laser-induced plasma images above the workpieces with the activating fluxes present different degrees of shrinkage compared with the uncoated one. A complicated interaction and energy coupling relationship exist among the laser-induced plasma, laser and weldment. The laser-induced plasma generally shows a negative effect in the laser welding process. The reason is that the plasma mainly affects the laser in two aspects, i. e., the absorption and

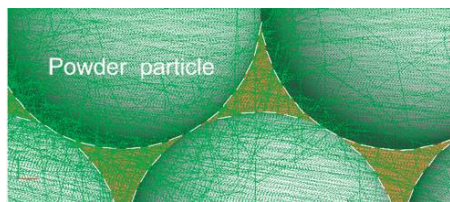


Fig.9 Multiple reflections between the spherical surfaces of the powder particles<sup>[19]</sup>

refraction. Since the plasma is an optically thinner medium with refractive index less than 1<sup>[20]</sup>, divergence will occur when the laser passes through, which is referred to as the “negative lens effect” of laser-induced plasma. The laser absorption reduces the laser power acting on the weldments, while the negative lens effect also reduces the laser power density on the weldments due to the enlargement of the laser spot diameter. Therefore, their combined effect leads to the decrease in the laser power density acting on the weldment<sup>[21]</sup>. The magnitude of absorption and refraction is related to the laser wavelength. The absorption action plays a dominant role when the wavelength is longer, while the refraction action becomes stronger when the wavelength is shorter<sup>[22]</sup>. According to Xiao<sup>[21]</sup>, compared with absorption, the negative lens effect of the plasma is the main mechanism of plasma shielding, and the wavelength of fiber laser is shorter ( $\lambda=1.06 \mu\text{m}$ ); thus the main effect of fiber laser-induced plasma on the laser is scattering. The magnitude of the scattering effect depends on the area of the plasma. The larger the area, the stronger the scattering effect<sup>[20]</sup>. Therefore, by reducing the area of the plasma, the activating fluxes can reduce the divergence of the laser beam so as to increase the absorption power density of the weld. Similar to the interaction between activating fluxes and free electrons in the arc plasma in A-TIG welding<sup>[23]</sup>, during active laser welding, the activating flux atoms evaporate after being heated by the laser, and then move to the plasma space to capture free electrons and form negative particles which disappear in the atmosphere, resulting in the reduction of the electron density of the plasma. According to Gao's research<sup>[16]</sup>, both CaF<sub>2</sub> and NaF can shrink TIG welding arc. Na<sub>2</sub>SiF<sub>6</sub> will undergo the following decomposition reaction at 300 °C:  $\text{Na}_2\text{SiF}_6=2\text{NaF}+\text{SiF}_4$ . SiF<sub>4</sub> is gaseous at room temperature<sup>[24]</sup>, and the generated NaF can also reduce the area of laser-induced plasma. The laser-induced plasma is formed by the evaporation and ionization of either the weld metal or shielding gas caused by the laser. According to the research of Yao<sup>[25]</sup>, the laser-induced plasma can be regarded as a point source heating the weldment in the form of thermal radiation. As a result, the shrinkage of plasma area leads to the reduction of heated area on the fusion zone surface, and further decreases the top weld width.

At present, another explanation of the activating fluxes influencing weld formation is that activating fluxes change the direction of Marangoni convection in the fusion zone. This theory is proposed to explain the mechanism of A-TIG welding penetration addition. When A-TIG is performed, some elements of the activating fluxes will cause the temperature gradient coefficient  $d\sigma/dT$  of the fusion zone surface tension to change from negative to positive, and the fusion zone flows from the edge to the center, forming a deep and narrow weld, as shown in Fig.11<sup>[26]</sup>.

The research of Heiple et al<sup>[27]</sup> indicates that the O and S are the main elements that change the temperature gradient coefficient of surface tension. Based on these facts, the elemental composition of the activating flux-coated weld was measured by energy spectrum, as shown in Fig.12. The results

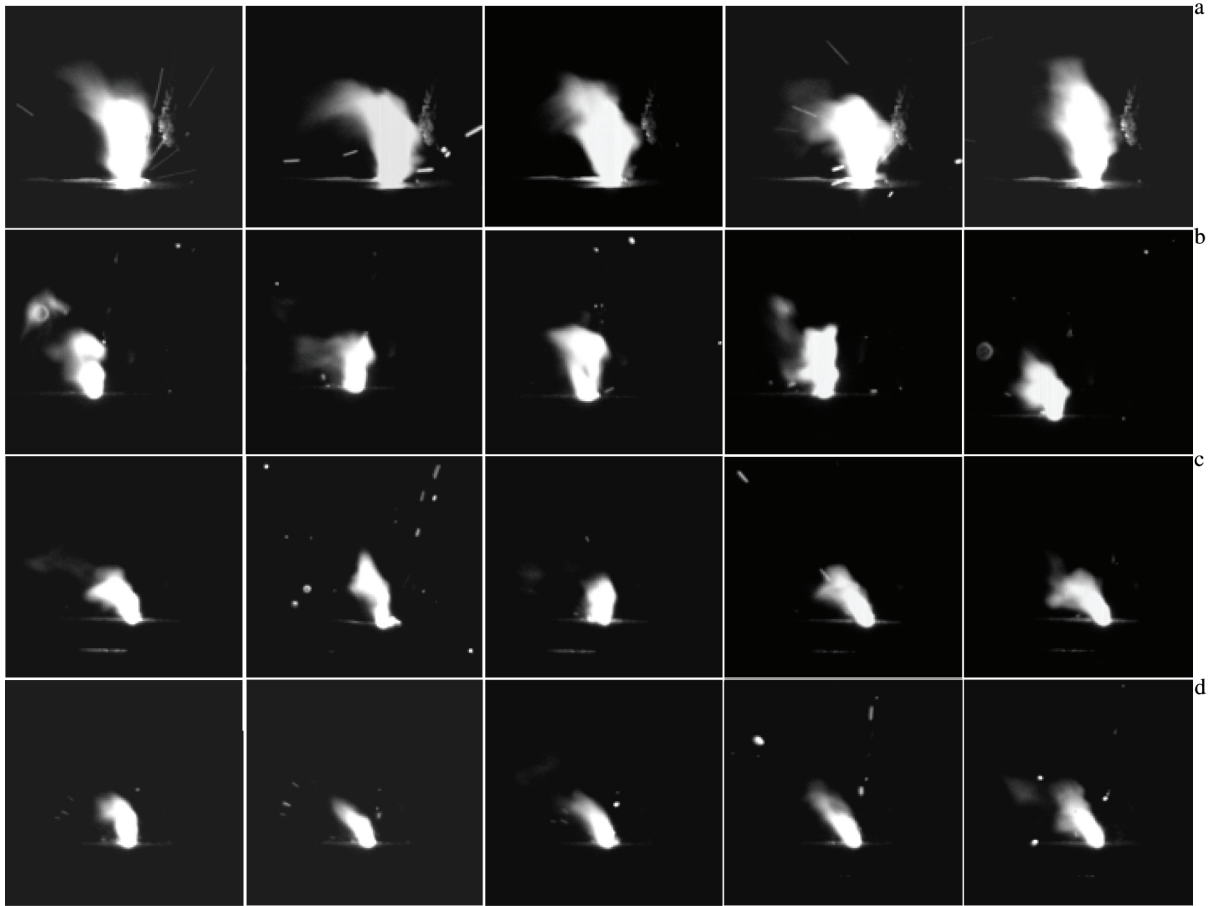


Fig.10 Morphologies of plasma under different conditions: (a) no flux, (b)  $\text{CaF}_2$ , (c)  $\text{NaF}$ , and (d)  $\text{Na}_2\text{SiF}_6$

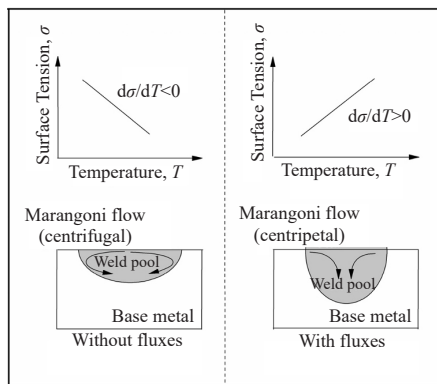


Fig.11 Schematic diagram of Marangoni convection theory<sup>[26]</sup>

indicate that the elements O and S are not detected, nor are other elements except for Ti, Al and V, which are the main constituent elements of the TC4 matrix. Therefore, the test results indicate that the chosen activating fluxes will not affect the weld formation by changing the convection direction of the fusion zone.

### 2.3 Microstructure of welds

Fig.13 demonstrates the microstructures of the upper part of the penetrated welds. As indicated in the welds coated with

$\text{CaF}_2$  and  $\text{NaF}$ , the  $\beta$  columnar crystals on the upper part of the welds grow towards weld surface, which seems the same as that of the welds without activating fluxes. Meanwhile, the columnar crystals of the upper part of the weld are oriented towards the weld center for the weld coated with  $\text{Na}_2\text{SiF}_6$ . These results are related to the width and shape of the upper fusion zone of the welds, because the columnar crystals of the fusion zone grow towards the maximum direction of heat dissipation (perpendicular to the fusion line and pointing to the center of the weld). Fig.14 shows the shape of the upper part of the weld.

Fig.15 shows the microstructures of the lower part of the welds. It can be seen that there is no obvious difference in the microstructure of the lower part of the welds. Fig.15 also shows that the lower part of the weld is more inclined to porosity, and the  $\text{CaF}_2$  coated weld is more prone to porosity compared with other two activating fluxes coated. The  $\beta$  columnar crystals in the laser welding of TC4 titanium alloy are mainly composed of acicular martensite  $\alpha'$ . According to the results shown in Fig.12, the constituent elements in the welds are evenly distributed in the columnar crystal, and no element enrichment is found at the grain boundary, which also indicates the characteristics of non-diffusion transformation of titanium martensite. The measurement results show that the

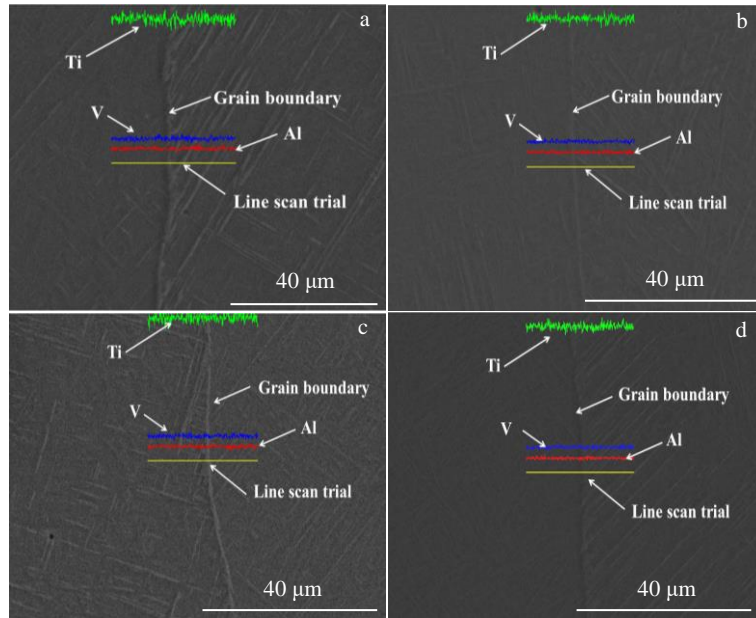


Fig.12 Element composition of weld at 3500 W: (a) no flux, (b)  $\text{CaF}_2$ , (c)  $\text{NaF}$ , and (d)  $\text{Na}_2\text{SiF}_6$

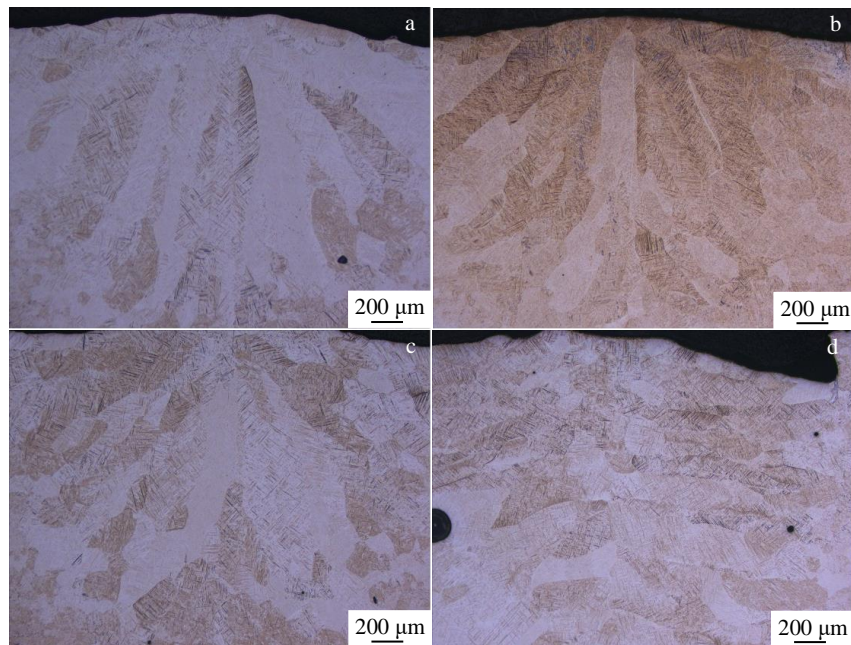


Fig.13 Microstructures of upper part of the weld at 3500 W: (a) no flux, (b)  $\text{CaF}_2$ , (c)  $\text{NaF}$ , and (d)  $\text{Na}_2\text{SiF}_6$

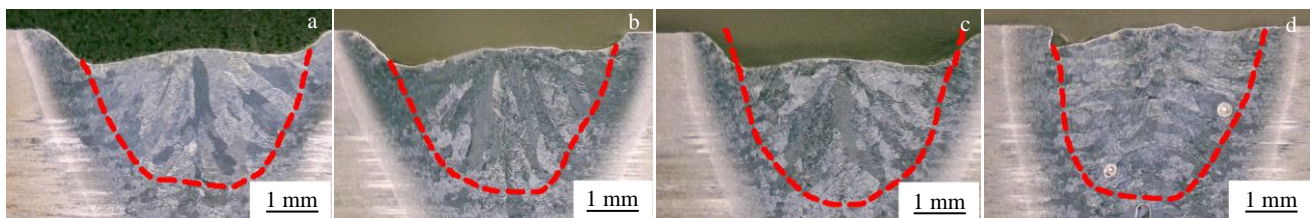


Fig.14 Weld morphologies of upper part of welds at 3500 W: (a) no flux, (b)  $\text{CaF}_2$ , (c)  $\text{NaF}$ , and (d)  $\text{Na}_2\text{SiF}_6$

average length of the columnar crystals on the upper part of the weld without activating fluxes is 1269  $\mu\text{m}$ , and that of weld with  $\text{CaF}_2$ ,  $\text{NaF}$  and  $\text{Na}_2\text{SiF}_6$  is 1132, 1036 and 995  $\mu\text{m}$ , respectively. The average length of the columnar crystals on the lower part of the weld without activating fluxes is 586  $\mu\text{m}$ , and that of weld with  $\text{CaF}_2$ ,  $\text{NaF}$  and  $\text{Na}_2\text{SiF}_6$  is 511, 578 and 644  $\mu\text{m}$ , respectively.

Fig.16 presents the morphologies of the acicular martensite  $\alpha'$  inside the columnar crystals on the upper part of the weld

obtained by EBSD. It also shows that compared with the weld without activating flux, the acicular martensite  $\alpha'$  morphology on the upper part of the weld with  $\text{CaF}_2$  is not obvious, and it is thinner in the weld with  $\text{NaF}$  coating. The acicular martensite  $\alpha'$  in the weld with  $\text{Na}_2\text{SiF}_6$  becomes shorter and thinner, which presents more obvious change compared with welds coated with  $\text{CaF}_2$  and  $\text{NaF}$ .

The weld microstructure refinement is related to rise in weld temperature due to the increase of laser absorption.

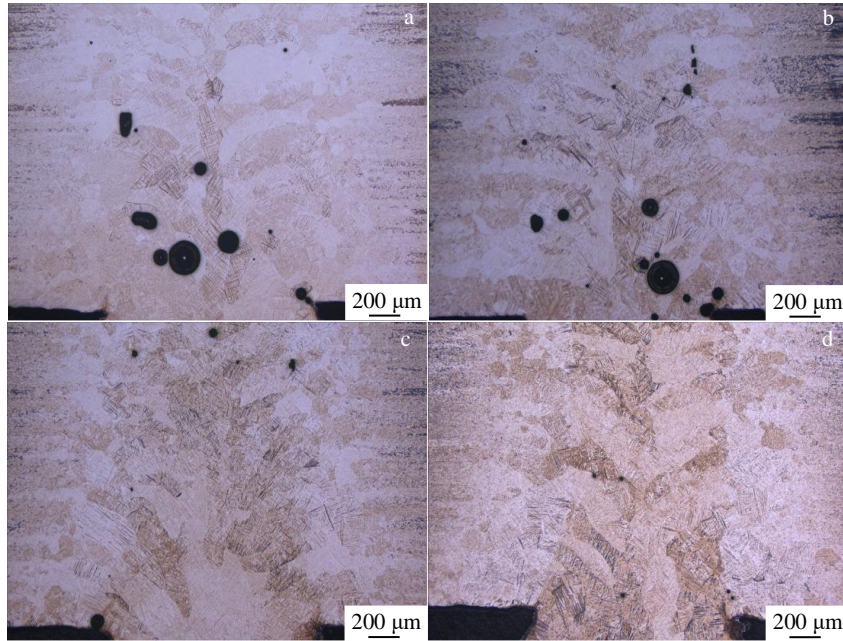


Fig.15 Microstructures of lower part of the weld at 3500 W: (a) no flux, (b)  $\text{CaF}_2$ , (c)  $\text{NaF}$ , and (d)  $\text{Na}_2\text{SiF}_6$

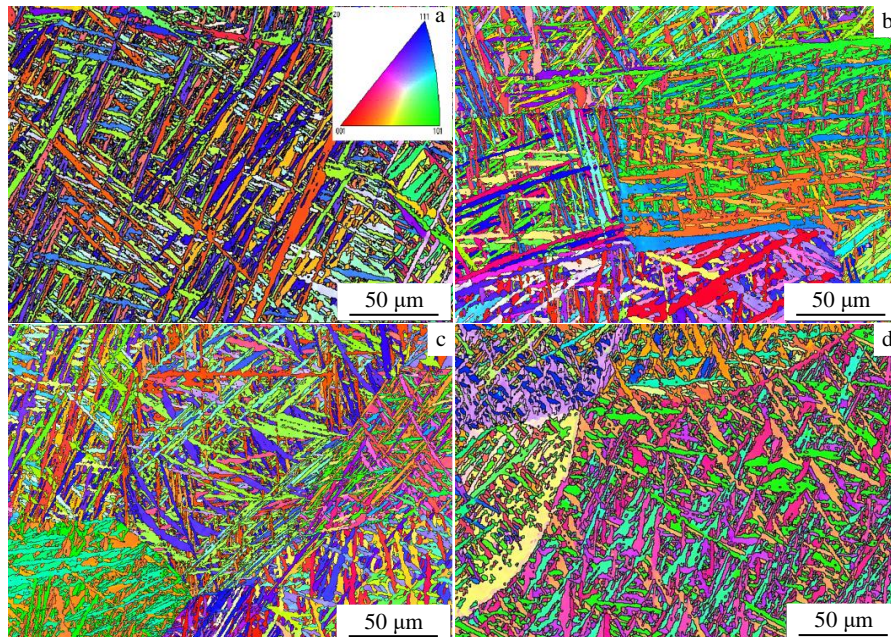


Fig.16 EBSD micrographs of  $\alpha'$  in weld  $\beta$  grains at 3500 W: (a) no flux, (b)  $\text{CaF}_2$ , (c)  $\text{NaF}$ , and (d)  $\text{Na}_2\text{SiF}_6$

According to the weld cooling rate formula<sup>[28]</sup>, temperature has a significant effect on the crystallization rate of molten metal. When other parameters remain unchanged, and the cooling rate increases, the grain growth time is shortened, so the weld microstructure is refined.

$$R = 2\pi K\rho C_p \left(\frac{vt}{q}\right) (T - T_0)^3 \quad (1)$$

where  $R$  is the cooling rate ( $^{\circ}\text{C/s}$ );  $K$  is the Boltzmann constant ( $\text{J/k}$ );  $\rho$  is the material density ( $\text{g/cm}^3$ );  $C_p$  is the specific heat capacity ( $\text{J}/(\text{cm}^3 \cdot ^{\circ}\text{C})$ );  $v$  is the welding speed ( $\text{cm/s}$ );  $t$  is the plate thickness ( $\text{mm}$ );  $q$  is the heat dissipation rate ( $\text{J/s}$ );  $T$  is the weld temperature ( $^{\circ}\text{C}$ );  $T_0$  is the base metal temperature ( $^{\circ}\text{C}$ ).

### 2.4 Properties of welded joints

The hardness distribution curve of the welded joints is shown in Fig. 17. The hardness of the welds zone (WZ) is higher than that of the heat affected zone (HAZ) and base metal (BM) since the microstructure of the welds is composed of titanium martensite  $\alpha'$  phase. The hardness of the weld with  $\text{Na}_2\text{SiF}_6$  is higher than that with  $\text{CaF}_2$  and  $\text{NaF}$ . There is no significant difference in the hardness of HAZ, indicating that the activating fluxes have no obvious effect on the microstructure of the HAZ.

The tensile strength of welded joints is shown in Table 1. It can be seen that the tensile strength of the welded joints is improved to varying degrees after coating with activating fluxes. The tensile strength of the joint coated with  $\text{Na}_2\text{SiF}_6$  is increased by 12.5%. It is related to the change of weld formation and microstructure with activating fluxes.

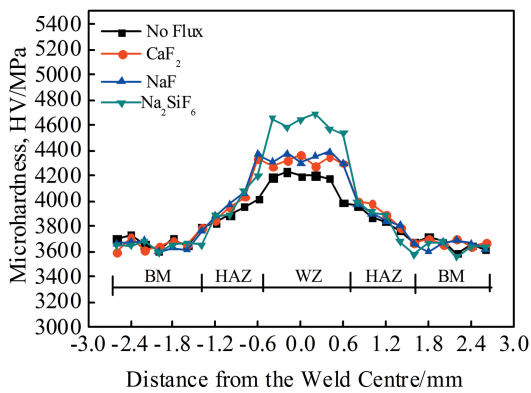


Fig.17 Microhardness distribution of welded joints with and without activating fluxes

Table 1 Tensile properties of welded joints

Activating flux	Tensile strength, $R_m$ /MPa	Fracture location
No	848	WZ
$\text{CaF}_2$	887	WZ
$\text{NaF}$	902	WZ
$\text{Na}_2\text{SiF}_6$	954	WZ

### 3 Conclusions

1)  $\text{CaF}_2$ ,  $\text{NaF}$  and  $\text{Na}_2\text{SiF}_6$  have no obvious effect on the weld surface formation. Different activating fluxes can not only increase the area of weld melting zone of TC4 titanium alloy to different levels since they can increase the laser absorptivity, but also demonstrate different degrees of effects on the dimension of both unpenetrated and penetrated weld formation, and amongst them,  $\text{Na}_2\text{SiF}_6$  has the most obvious effect on the weld formation.

2) The increase of laser absorptivity is relevant to the change of TC4 weldment surface status and compressing of laser-induced plasma area caused by activating fluxes. The decrease of top weld width has a certain relation to the shrinkage of laser-induced plasma. The activating fluxes have no effect on the Marangoni convection direction of the fusion zone.

3) For the welds coated with  $\text{CaF}_2$ ,  $\text{NaF}$  and without activating fluxes, the  $\beta$  columnar crystals on the upper part of the welds all grow towards the weld surface. For the welds coated with  $\text{Na}_2\text{SiF}_6$ , the  $\beta$  columnar crystals on the upper part of the welds grow towards the weld center. The activating fluxes have no obvious effect on the growing direction of the  $\beta$  columnar crystals on the lower part of the weld.  $\text{Na}_2\text{SiF}_6$  can significantly refine the acicular  $\alpha'$  in the  $\beta$  columnar crystals on the upper part of the welds in the laser welding of TC4 alloy.

4) The tensile strength of the welded joint coated with  $\text{Na}_2\text{SiF}_6$  is increased by 12.5%. Compared with other two activating fluxes,  $\text{Na}_2\text{SiF}_6$  has the most prominent effect on the weld formation and mechanical property in the laser welding of TC4 titanium alloy, and thus it can be used as the most preferred activating flux.

### References

- 1 Antunes R A, Salvador C A F, Oliveira M C L. *Materials Research*[J], 2018, 21(2): 1
- 2 Osorio G C, Valencia A M J, Agualimpia C M et al. *Revista Facultad de Ingenieria*[J], 2018, 27(18): 17
- 3 Gorynin I V. *Materials Science and Engineering*[J], 1999, (A263): 112
- 4 Qi Y L, Deng J, Hong Q. *Materials Science and Engineering*[J], 2000, 280: 177
- 5 Balasubramanian T S, Balakrishnan M, Balasubramanian V et al. *Science and Technology of Welding and Joining*[J], 2011, 16(8): 702
- 6 Kaul R, Ganesh P, Singh N et al. *Science and Technology of Welding and Joining*[J], 2007, 12(2): 126
- 7 Kuo M, Sun Z, Pan D. *Science and Technology of Welding and Joining*[J], 2001, 6(1): 16
- 8 Shan J G, Zhang T, Ren J L. *Transaction of the China Welding Institution*[J], 2008, 29(2): 8 (in Chinese)
- 9 Parshin S G, Parshin S S, Burkner G et al. *Welding International* [J], 2011, 25(7): 545

- 10 Cretteur L, Marya S. *Welding International*[J], 2000, 14(2): 120
- 11 Qin G L, Wang G G, Zou Z D. *Trans Nonferrous Met Soc China* [J], 2012, 22: 23
- 12 Sun H, Zhang Z D, Liu L L. *Transaction of the China Welding Institution*[J], 2007, 28(4): 49 (in Chinese)
- 13 Shen J, Wang L Z, Zhao M L et al. *Science and Technology of Welding and Joining*[J], 2012, 17(8): 665
- 14 Xie J L, Chen Y H, Yue Z Z. *High Power Laser and Particle Beams*[J], 2015, 27(2): 1
- 15 Gao X G, Dong J H, Han X et al. *Transaction of the China Welding Institution*[J], 2017, 38(7): 31 (in Chinese)
- 16 Gao X G, Dong J H, Han X. *Transaction of the China Welding Institution*[J], 2017, 38(10): 31 (in Chinese)
- 17 Yang Q L. *Journal of Dalian Jiaotong University*[J], 2012, 33(2): 81
- 18 Zhang J Y, Gu D D, Yang Y et al. *Engineering*[J], 2019, 5(4): 736
- 19 Yang Y, Gu D D, Dai D H et al. *Materials and Design*[J], 2018, 143(5): 12
- 20 Zhao L L, Tang Z, Li G H et al. *Applied Laser*[J], 2007, 27(5): 357 (in Chinese)
- 21 Xiao R S, Chen K, Chen J M et al. *Laser Technology*[J], 2001, 25(3): 238 (in Chinese)
- 22 Tang X H, Zhu H H, Zhu G F et al. *Journal of Huazhong Univ of Sci & Tech*[J], 1996, 24(6): 54 (in Chinese)
- 23 Tanaka M, Shimizu T, Terasaki H et al. *Science and Technology of Welding and Joining*[J], 2000, 5(6): 397
- 24 Cai M, Tang A J, Wang L S et al. *Bulletin of the Chinese Ceramic Society*[J], 2017, 36(3): 859 (in Chinese)
- 25 Yao W, Gong S L, Chen L. *Transaction of the China Welding Institution*[J], 2004, 25(5): 74 (in Chinese)
- 26 Gao X G, Dong J H, Han X. *Int J Adv Manuf Technol*[J], 2017, 91(1): 1181
- 27 Heiple C R, Roper J R. *Welding Research Supplement*[J], 1981(8): 143
- 28 Wang W. *Modern Welding Technology*[J], 2009(1): 15 (in Chinese)

## TC4钛合金活性激光焊焊缝成形及组织性能

侯继军, 董俊慧, 许爱平

(内蒙古工业大学 材料科学与工程学院, 内蒙古 呼和浩特 010051)

**摘要:** 选取 $\text{CaF}_2$ 、 $\text{NaF}$ 和 $\text{Na}_2\text{SiF}_6$ 作为活性剂对TC4钛合金进行活性激光焊接, 在焊接过程中利用高速摄像机采集焊件上方的光致等离子体图像, 焊后借助光学显微镜测量焊缝熔深和熔宽, 利用EBSD观察分析焊缝显微组织, 采用能谱仪测试焊缝元素组成, 测试接头硬度和抗拉强度。结果表明, 由于活性剂改变了焊件表面状态和压缩光致等离子体面积从而提高了激光吸收率, 这使得焊缝熔化区面积增加; 活性剂均可以使未熔透焊缝的熔深增加, 正面熔宽减小, 熔透焊缝正面熔宽减小, 中部和背面熔宽均增加, 3种活性剂中 $\text{Na}_2\text{SiF}_6$ 对TC4钛合金激光焊焊缝成形的影响最明显; 活性剂对焊缝下部显微组织影响不大, 涂敷 $\text{CaF}_2$ 和 $\text{NaF}$ 后, 焊缝上部 $\beta$ 柱状晶的生长方向与未涂敷焊缝 $\beta$ 柱状晶生长方向都指向焊缝表面, 涂敷 $\text{Na}_2\text{SiF}_6$ 焊缝上部 $\beta$ 柱状晶的生长方向指向焊缝中心。涂覆 $\text{CaF}_2$ 焊缝针状马氏体 $\alpha'$ 形态变化不明显, 涂敷 $\text{NaF}$ 的针状马氏体 $\alpha'$ 变得稍细, 而涂敷 $\text{Na}_2\text{SiF}_6$ 的针状马氏体 $\alpha'$ 变得短且细, 较涂敷 $\text{CaF}_2$ 和 $\text{NaF}$ 的焊缝变化最明显。涂敷 $\text{Na}_2\text{SiF}_6$ 的接头抗拉强度提高约12.5%, 从改善焊缝成形和提高接头力学性能考虑,  $\text{Na}_2\text{SiF}_6$ 可作为TC4钛合金激光焊的首选活性剂。

**关键词:** 活性剂; TC4; 焊缝成形; 显微组织; 力学性能

**作者简介:** 侯继军, 男, 1985年生, 博士生, 讲师, 内蒙古工业大学材料科学与工程学院, 内蒙古 呼和浩特 010051, E-mail: 393442628@qq.com